Small scale intermittency and bursting in a turbulent channel flow

Miguel Onorato
Dipartimento di Fisica Generale, Università di Torino, Via Pietro Giuria 1, 10125 Torino, Italy

Roberto Camussi
Dipartimento di Ingegneria Meccanica e Industriale, Università Roma Tre, Via della Vasca Navale 79, 00146 Roma, Italy

Gaetano Iuso
Dipartimento di Ingegneria Aerospaziale, Politecnico di Torino, Corso Duca degli Abruzzi 24, 10129 Torino, Italy
(Received 25 May 1999; revised manuscript received 5 October 1999)

The statistical properties of the streamwise velocity fluctuations in a fully developed turbulent channel flow are studied experimentally by means of single hot wire measurements. The intermittency features, studied through the scaling of the moments of the velocity structure function computed using the extended self-similarity and through the probability density function of the wavelet coefficients, are found to be dependent on the distance from the wall. The maximum intermittency effects are observed in the region between the buffer layer and the inner part of the logarithmic region where it is known that the bursting phenomenon, related to coherent structures such as low speed streaks and streamwise vortices, is the dominant dynamical feature. An eduction technique based on wavelet transform for identification of organized motion is developed and used to analyze the turbulent signals. Streamwise velocity conditional averages computed on events educed with the proposed method are reported. Events responsible for intermittency are found to consist of regions of high velocity gradients and are directly correlated with the observed increase of intermittency close to the wall.

PACS number(s): 47.27.Nz, 01.50.Pa

I. INTRODUCTION

A. Background

During the past few years there has been a lot of interest in the study of the statistical properties of homogeneous and isotropic turbulent flows and nowadays it is well accepted that scaling exponents of the p moments of velocity structure function (hereafter denoted as ζ_p) are nonlinear functions of p (see, e.g., Ref. [1]). The nonlinearity of the scaling exponents, also known as anomalous scaling, has been observed by many experimental investigations [2,3], and confirmed by numerical simulations [4]. This anomalous scaling, related to the change of the shape of the probability density function (PDF) of the velocity difference for different scales (from a quasi-Gaussian PDF for large scales to a distribution with exponential tails for small scales), has been associated with small scale intermittency which basically consists of an uneven distribution of the turbulent energy rate of dissipation. In parallel with these studies, numerical simulations [5,4] revealed, in isotropic turbulence, the presence of filamentary structures associated with high velocity gradients. From the theoretical viewpoint, a statistical model that takes into account the presence of organized filamentlike structures has been proposed by She and Léveque [6] and their prediction of the scaling exponents is in good agreement with experiments in homogeneous and isotropic turbulence. However, the nature of organized structures, their role in the mechanism of turbulent energy dissipation, and their connection with anomalous scaling are aspects not yet clear mainly in real turbulent flows where inhomogeneous and unisotropic conditions are encountered.

Indeed, most of the experimental work performed so far on the scaling of the velocity structure functions has been conducted in almost isotropic turbulent flows; less attention has been paid to the case of nonisotropic and inhomogeneous conditions where it is well know that large scale organized structures exist and can be dynamically important (see, for example, Ref. [7]). Only recently, scaling exponents for non-homogeneous and nonisotropic cases have been determined experimentally by Camussi *et al.* [8] very close to a grid, by Protas *et al.* [9] and Gaudin *et al.* [10] in wakes, by Chillá and Pinton [11] in a closed von Karman flow, by Amati *et al.* [12] and Antonia *et al.* [13] in a numerical and experimental channel flow. Most of the results agree on the fact that the ζ_p deviation from linearity is much more evident in cases where anisotropy is present and this phenomenon is presumed to be associated with passages of coherent structures.

This aspect has particular importance in the case of boundary layer flows in connection with the typical bursting process which is relevant for many practical reasons (energy budgets, turbulent production, drag reduction, or heat transfer properties). Especially after the DNS results, it has become increasingly clearer that the dynamics and the instabilities of low speed streaks in the wall region are responsible for the bursting process in the turbulent boundary layer [14,15]. Indeed, as indicated by Sandborn in 1959 [16], who analyzed band passed signals acquired in a turbulent boundary layer, the presence of low speed streaks might be indicated by ''bursts in the over all (all frequencies) hot wire signal.'' Successive experimental studies were performed in order to develop methods for localizing the bursting events from a time series and to have a better understanding of their relation to small scale intermittency [17–19].

In the present work, an experimental study of the streamwise velocity fluctuations statistics in a turbulent channel flow has been performed. The main task is to analyze how intermittency and scaling anomalies are modified by the presence of the wall and to correlate the observed behaviors

to the bursting process typical of the boundary layer flows.

The experiment has been carried out in an air channel flow placing a single hot wire probe at different distances from the wall. The Reynolds number in the experiment was not large enough to achieve an inertial range sufficiently wide for the computation of the ζ_p. Therefore, the extended self-similarity (ESS) form of scaling, proposed by Benzi *et al.* [20], has been used to determine scaling ranges and for the accurate calculation of the intermittency exponents. Statistical analysis is also performed using the wavelet decomposition of the streamwise velocity signals. Due to the correspondence between wavelet coefficients and velocity difference, of interest is the analysis of the scaling properties and of the PDF of the wavelet coefficients computed at different scales and at several distances from the wall. In order to correlate the anomalous scaling of the wavelet coefficients (or of the velocity difference) with the intermittency phenomenon, a method for turbulent events eduction has been developed. The technique, inspired by previous works of Farge *et al.* [21] and Camussi and Guj [22], is based on the wavelet transform. With respect to previous methods which rely on the imposition of a more or less arbitrary threshold, in the present approach it is assumed that the turbulent flows structures are the main features responsible for the non-Gaussian PDF of the wavelet coefficients and, on this basis, a threshold is automatically selected. Our method is based on the assumption that non-Gaussian statistics are a signature of some coherence in turbulence, in contrast to systems with random interactions which give Gaussian statistics according to the law of large numbers [23]. Turbulent events are then identified and their relations to the anomalous scaling are discussed. Further details on the ESS technique and on the proposed method for turbulent event eduction are presented in the next subsections. In Sec. II, the experimental setup is described whereas Sec. III contains the results and discussions. Final remarks and conclusions are reported in Sec. IV.

B. ESS and wavelet decomposition

As pointed out above, anomalous scalings in the inertial range are related to the intermittent nature of the turbulent energy dissipation. The intermittency effects on the scaling of the structure functions can be determined if an inertial range is present and sufficiently extended. For most of the experimental facilities, since a very high Reynolds number is not so easily achievable, the inertial range is limited to a narrow band of scales, making the study of intermittency rather difficult. The introduction of the ESS allows the study of scaling laws at moderate and low Reynolds number to be performed. ESS consists of representing the pth order structure function as a function of the third order one. Formally this reduces to

$$S_p(r) \sim S_3(r)^{\zeta_p^*}, \tag{1}$$

where ζ_p^* is known as the relative scaling exponent in contrast to the absolute scaling exponent ζ_p; $S_p(r)$ is the structure function computed with the absolute value of the velocity difference (for a discussion on the use of the absolute value, see Refs. [24,25]):

$$S_p(r) = \langle |u(x+r) - u(x)|^p \rangle \sim r^{\zeta_p}. \tag{2}$$

The Kolmogorov theory [26], which does not account for intermittency of energy dissipation, predicts a linear dependence of ζ_p upon p and precisely, $\zeta_p = p/3$. The advantage of using Eq. (1) instead of the method of Eq. (2) is straightforward: the range where a scaling law applies is wider, allowing a good fit for the determination of the scaling exponents. Furthermore, the scaling exponents obtained by ESS have been demonstrated experimentally to be in good agreement with the scaling found in experiments at very high Reynolds number computed in the standard way [3].

As it will be shown later, due to the direct connection with the velocity differences, the application of the ESS to the wavelet coefficients obtained by the wavelet decomposition of the velocity signals is also straight forward. Here we very briefly review some properties of the wavelet transform which are fundamental in the successive analysis. Wavelet coefficients are defined as follows (see Ref. [27] for details):

$$w(r,x) = \frac{1}{r} \int \psi^*((x'-x)/r) u(x') dx', \tag{3}$$

where ψ is the wavelet function (ψ^* is the complex coniugate), $u(x)$ is the signal to be analyzed, and r corresponds to a scale. The wavelet transform is capable of revealing scaling laws: It can be proved [27] that when the structure function of a signal behaves as a power law, then also the wavelet coefficients scale as a power law and the following relation applies:

$$\langle w(r,x) \rangle_x \sim r^{\alpha}, \tag{4}$$

where α is the scaling exponent and the symbol $\langle \ldots \rangle_x$ denotes an average over the positions x. As will be clearer later, Eq. (4) is very suitable for calculating the conditional scaling exponent by averaging only on preselected x. If the moments of the wavelet coefficients are plotted as functions of the third order moment of the wavelet coefficients instead of as a function of the scale r, a sort of ESS for wavelet coefficients is achieved, rendering the wavelet scaling analysis possible even at low Reynolds number.

From wavelet coefficients, qualitative indicators of intermittency can be defined. An interesting measure of intermittency has been introduced by Farge [27] and Farge *et al.* [21] and is defined as follows:

$$I(r,x) = \frac{|w(r,x)|^2}{\langle |w(r,x)|^2 \rangle_x}, \tag{5}$$

which gives an unambiguous characterization of the local activity of the velocity field at each scale.

A second indicator of intermittency is the flatness factor of the wavelet coefficients:

$$F(r) = \frac{\langle w(r,x)^4 \rangle_x}{\langle w(r,x)^2 \rangle_x^2}. \tag{6}$$

For real wavelets, f_{FF} and f_{LIM} are strictly related: by squaring and averaging definition (5) over x, it follows that

$$F(r) = I(r,x)^2 \rangle_x. \tag{7}$$

The F and I represent the basic ingredients for the implementation of the present method of events eduction which is described in the following paragraph. The application of the

ESS technique to velocity data, and to the corresponding wavelet coefficients, at different distances from the wall will be presented in Sec. III.

C. Eduction criterion for events selection

In this paper we developed a method for individuating turbulent events using the wavelet transform which seems to be a natural tool for relating anomalous scaling, intermittency and bursting process (see [22,27,28]). The present technique is based on the paper by Camussi and Guj [22], who, starting from the definition (5) and using orthogonal wavelets, developed a method for individuating structures in a turbulent flow. Their method consists in selecting a scale r_0 and localizing portion of the signal where the value of the function I is greater than a preselected threshold. They have shown that physically this correspond to select, in the time series, the instants corresponding to passages of coherent structures.

In order to select systematically the events in all scales, we present a method for the selection of the threshold. We consider the I function but, instead of imposing an arbitrary threshold whose effect on statistical quantities is *a priori* unknown, we select it in such a way that the F for each scale is equal to 3. The method can be simply summarized as follows: we compute the flatness factor at each wavelet scale; if it is greater than 3, we impose a threshold on the I function and recalculated the flatness factor excluding those regions in which I is greater than the selected threshold. If the flatness factor is still greater than 3, the threshold is lowered and the process is iterated until a flatness factor of 3 is reached for all scales. If F is less than 3 for a given scale, events are not detected. The method selects as events those regions whose effect on the complete signal is to make the PDF of the wavelet coefficients strongly non-Gaussian in each scale. Usually smaller scales require a lower threshold. As will be shown in the next paragraph, the method allows us to divide the signal into two contributions: the first one, in which, by definition, all wavelet scales have the same quasi-Gaussian PDF and the second one, which is responsible for the anomalous scaling and includes only the events. It has to be remarked that F equals to 3 does not imply that the PDF is Gaussian since the PDF is univocally determined by all its moments, so the signal without events, even though has a $F=3$, is not necessarily strictly Gaussian.

Once the events have been localized, the original signal can be phase averaged, in order to obtain a ''mean signature event.''

II. EXPERIMENTAL SETUP AND FLOW PROPERTIES

The experiment has been carried out in a rectangular cross section channel, 7 m long, 70 mm high, and 300 mm wide, arranged in five Plexiglas modules. The channel is situated at the exit of a convergent, which in turn is located downstream from a settling chamber fitted by the fan section. To avoid the effects of the vibrations induced by the electric motor on the measurements in the test section, an annular rubber ring was interposed in between the fan section and the settling chamber. The whole duct was also insulated from the ground by inserting blocks of rubber between the ground itself and the channel steel supports. The upper surface of the channel was equipped with 35 static pressure taps connected to a *scanivalve* system in order to evaluate the pressure gradient, a Setra pressure transducer with amplified output signal was used for the pressure readings. Further details on the experimental set up may be found in Ref. [29].

The Reynolds number based on the mean velocity at the center of the channel and on the channel half height was 10 800 which corresponds to $\mathrm{Re}_\tau=510$ ($u_\tau=0.213$ m/s). In this condition, a fully developed flow was well assessed at a distance corresponding to 157 half channel heights downstream the inlet of the channel where measurements were taken. Longitudinal velocity measurements have been performed using a single subminiature hot wire sensor (probe type DANTEC 55A53) characterized by 2 μm of diameter and 0.45 mm long, which corresponds to 6.6 wall units, low enough to obtain a good spatial resolution in the turbulence measurements near the wall [30]. The probe was connected to a CTA Dantec 55C01/C10 Bridge. *In situ* calibrations were carried out before and after each set of measurements and data were discarded if any significant difference in the calibration curve was present. Direct current offset voltage was applied to the signal before amplification of the alternating part in order to cover the complete dynamic range of the analog-digital (A/D) converter. Preliminary power spectra were performed using a Bruel-Kjear spectrum analyzer in order to have indications of the maximum frequencies containing significant energy contribution. Time series of 230 000 data sampled at 6 kHz were collected using a 12-bit A/D data acquisition system and anti-aliasing filtering was performed by an analog filter (roll off 80 dB/decade) at a frequency cutoff of 3 kHz. It has to be pointed out that due to the relatively small frequency sampling, the dissipative range is not well resolved but a sufficiently large number of statistically independent samples is acquired. Indeed, close to the wall, the typical scale of an eddy may be estimated to be of the order of 25 viscous lengths, the diameter of the streamwise vortices (see, e.g., Ref. [14]). Therefore the total acquisition time window corresponds to more than 5×10^3 eddy turnover times. Using this value as an estimation of the number of independent samples, the maximum order p that may be computed for a reliable computation of the ζ_p corresponds to about $p_{max}=6$ (see Ref. [31]). Therefore, this is the limit we assume for the following analyses. Note also that the use of the ESS improves the statistical convergence (see Ref. [32]) as well as the use of the wavelet coefficients which are less affected by the background noise [22]. In the case of positions far from the wall, the flow may be considered quasi-isotropic. Therefore, an estimation of the eddy turnover time may be computed on the basis of the Taylor microscale [31]. In this case, the number of independent samples results again to be of the order of 5×10^3 and therefore the above considerations on the reliability of the moments of the velocity structure functions still apply.

The probe positioning was performed by a micropositioner characterized by an accuracy of ±0.005 mm which was mounted on the upper surface of the channel for the accurate location of the hot wire probe. Measurements were performed at different heights from the wall. In Fig. 1(a) we show the mean velocity profile in terms of the law of the wall (von Karman's constant $k=0.41$) compared with experimental data of Antonia *et al.* [33] at $\mathrm{Re}=11\,600$, and the

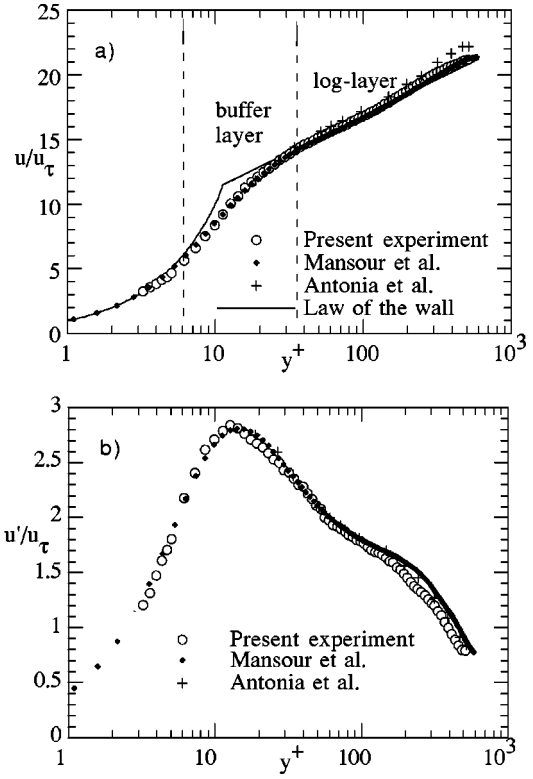

FIG. 1. Streamwise velocity mean profile (a), and rms (b), normalized with the velocity skin friction as a function of the distance from the wall y^+. Present experimental data are compared with results from numerical simulation by Mansour *et al.* at Re=10 935 and with the experimental data of Antonia *et al.* Re=11 600. In the plot is also reported the law of the wall.

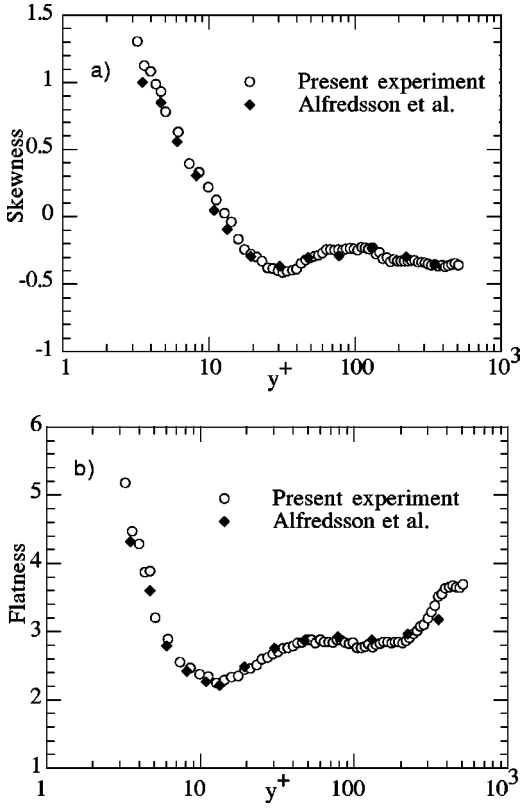

FIG. 2. Skewness (a), and flatness (b), of the streamwise velocity as a function of the distance from the wall y^+. Present experimental data are compared with experimental data from Alfredsson *et al.* at Re=7500.

numerical data of Mansour *et al.* [34] at Re=10 935; as can be seen from Fig. 1(a), a good agreement is achieved. In the same figure the regions corresponding to the buffer layer and the log-layer are also evidenced. The distribution of the turbulence intensity u'/u_τ (where u' denotes the streamwise velocity rms) as a function of the wall distance y^+ is displayed in Fig. 1(b) and compared to the numerical and experimental data cited above. In Figs. 2(a) and 2(b) higher order statistics, respectively, skewness and the flatness, are shown. On the same diagrams, to complete the validation of present flow conditions, data at Re=7500 from the literature [35] are also reported for comparison, showing good agreement.

III. RESULTS AND DISCUSSION

In this section results obtained by the application of the above described postprocessing methods are presented. In all the analysis the standard Taylor hypothesis has been used in order to convert time scales to space scales. The validity of the Taylor hypothesis for the calculation of the structure function in a turbulent channel flow has been discussed by Antonia *et al.* [36]. Data are first analyzed with no conditioning and the ESS is applied to both the raw data and to the corresponding wavelet coefficients. In this way we try to define which region of the boundary layer shows larger intermittency. Then, the connection with the bursting process is analyzed statistically by using the events eduction criterion. The achieved results are discussed in the frame of the possible physical interpretations mainly concerning the different behaviors observed for different distances from the wall.

A. Statistical analysis with no conditioning

Figure 3 shows the dependence of the third order structure function on the scale r^+ at $y^+=15$ and $y^+=310$. As expected, there is no evidence of an inertial range, therefore the ESS was employed to characterize the anomalous scaling. In Figs. 4 and 5, we show some examples of the ESS results obtained by plotting the fourth and sixth order structure func-

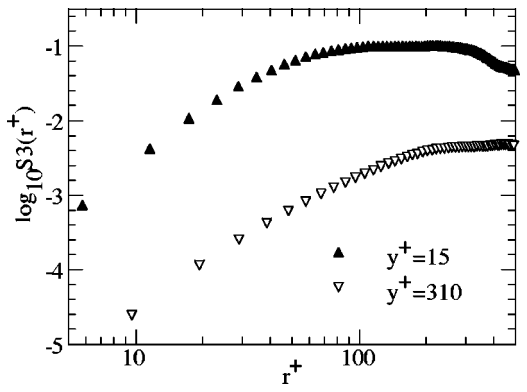

FIG. 3. Third order structure function at $y^+=15$ and at $y^+=310$. There is no evidence of an inertial range.

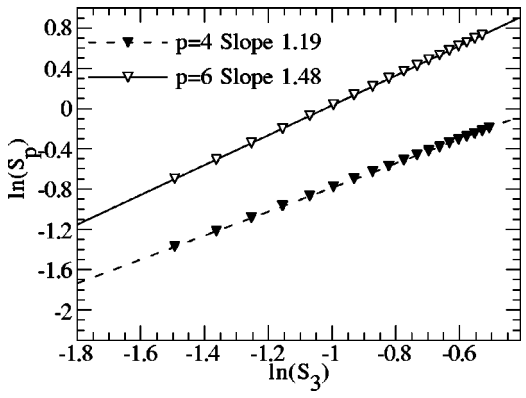

FIG. 4. Fourth and sixth order moment of the velocity structure function at $y^+=15$ as a function of the third order structure function. The structure functions are represented by the symbols and the fits by the dashed, $S_4(r)$, and solid, $S_6(r)$, lines. In the plot are also reported the slopes of the fits. The dissipative range is not included in the plot.

tions as a function of the third order one, as indicated by Eq. (1). Two cases, corresponding to two different distances from the wall, are considered: The first one (Fig. 4) corresponds to the buffer region ($y^+=15$) and the other (Fig. 5) to a position almost in the center of the channel ($y^+=310$). The smaller scale used for computing the scaling exponent has been determined by looking at the region where the local slope of $\ln[S_6(r)]$ vs $\ln(S_3(r))$ as a function of y^+ becomes constant. The upper bounds have been selected by the integral scale calculated through the autocorrelation function. In both figures the dissipative range and the scales greater than the integral 1 are not reported.

The first comment to be underlined here is that, either close to the wall where the viscosity surely plays an important role at all the scales, and almost at the center of the channel, a scaling region (in the ESS representation) can be defined. Therefore, even if the dissipative range is not completely resolved, clear scaling is observed and the ζ_p can be computed accurately. Concerning the amplitude of the scaling exponents it is shown that at $y^+=310$, the values of ζ_4^*

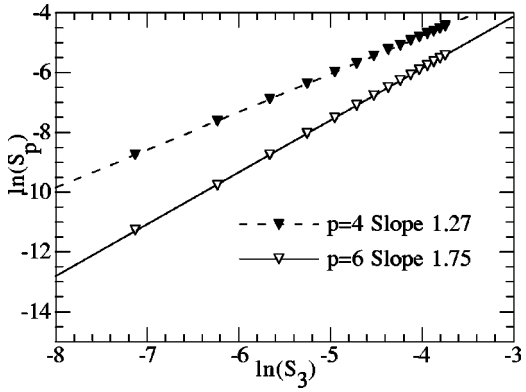

FIG. 5. Fourth and sixth order moment of the velocity structure function at $y^+=310$ as a function of the third order structure function. The structure functions are represented by the symbols and the fits by the dashed, $S_4(r)$, and solid, $S_6(r)$, lines. In the plot are also reported the slopes of the fits. The dissipative range is not included in the plot.

TABLE I. Relative scaling exponents for the She-Léveque model, for the present experimental turbulent channel flow at $y^+=310$ and at $y^+=15$. The scaling exponents have been calculated using the ESS.

p	ζ_p She-Léveque	ζ_p at $y^+=310$ present expt.	ζ_p at $y^+=15$ present expt.
1	0.37	0.37	0.43
2	0.70	0.70	0.75
3	1.00	1.00	1.00
4	1.28	1.27	1.19
5	1.54	1.52	1.34
6	1.78	1.75	1.48

and ζ_6^* are very close to the ones obtained in homogeneous turbulence ($\zeta_4^*=1.27$ and $\zeta_6^*=1.75$ compared to $\zeta_4^*=1.28$, $\zeta_6^*=1.78$ from Ref. [6]). On the other hand, a substantial difference is found at $y^+=15$ where the scaling exponents are $\zeta_4^*=1.19$ and $\zeta_6^*=1.48$. For a more quantitative analysis, the scaling exponents obtained for p ranging from 1 to 6, are also reported in Table I. The present analysis, therefore, confirms that there is an increase of intermittency for decreasing distances from the wall and this effect is revealed by the stronger ζ_p anomalies observed for decreasing y^+.

In order for this point to be better understood, the scaling exponent of the sixth order structure function across the normal direction of the channel has been analyzed in more detail. In Fig. 6 the so called intermittency parameter [2], $\mu=2-\zeta_6^*$, which gives the anomaly with respect to the Kolmogorov [26] linear prediction and that characterizes by the small scale intermittency, is shown as a function of y^+. The error bar has been evaluated by the standard deviation of the local derivative, computed over neighboring points, in the range where the scaling was detected. Figure 6 shows a peak at around $y^+=20$ and then μ decreases moving towards the center of the channel. For $y^+\geqslant 100$, within the log-layer, the intermittency factor is almost constant. At $y^+=310$ the intermittency parameter is $\mu=0.26$ in agreement with previous observations in isotropic and homogeneous turbulence (e.g. Ref. [2]). Similar results where found by Antonia *et al.* [13]

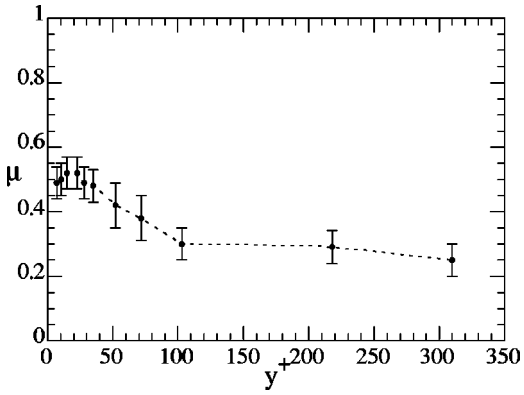

FIG. 6. Intermittency parameter as a function of the vertical coordinate y^+. The error bars are given by the standard deviation of the local relative scaling exponent calculated over neighboring points of the ESS representation.

TABLE II. Relative scaling exponents at $y^+=15$ calculated with ESS using the structure function and wavelet coefficients.

p	$\zeta_p y^+=15$	$\zeta_p y^+=15$ wavelet
1	0.43	0.41
2	0.75	0.75
3	1.00	1.00
4	1.19	1.19
5	1.34	1.35
6	1.48	1.49

from hot wire, laser Doppler anemometry, and DNS data, performed at $\mathrm{Re}_\tau=180$. The results confirm that a stronger intermittency is observed close to the wall and indicates also that the largest intermittency is revealed within the buffer region and, more precisely, in the range $10\leqslant y^+\leqslant 40$.

Analogous results are obtained when the ESS form of scaling is applied to the wavelet coefficients. In Table II, we report the value of scaling exponents computed using the ESS on the velocity signal, and with the wavelet coefficients at $y^+=15$.

To further investigate the intermittency nature of the streamwise velocity across the channel, we show in Figs. 7(a) and 7(b) the PDF of the wavelet coefficients at $y^+=310$ and $y^+=15$, computed respectively at scales $r^+=40$, 80, 200. The behavior is the typical one of a turbulent flow: for both distances [Figs. 7(a) and 7(b)], at large scales ($r^+=200$) the PDF's have a quasi-Gaussian distribution, while for intermediate and small scales the PDF's are characterized by increasingly wider tails. To better highlight the differences between the two regions, in Fig. 8 we compare the PDF at $y^+=310$ and $y^+=15$, computed at the same scale ($r^+=40$). The right part of the PDF overlaps almost perfectly, the left part instead is wider at $y^+=15$ in respect with $y^+=310$, indicating a more intermittent process in the buffer region. This result is consistent with the one obtained by Benzi *et al.* [37] in a numerical simulation of a channel flow (see Fig. 1 in their paper).

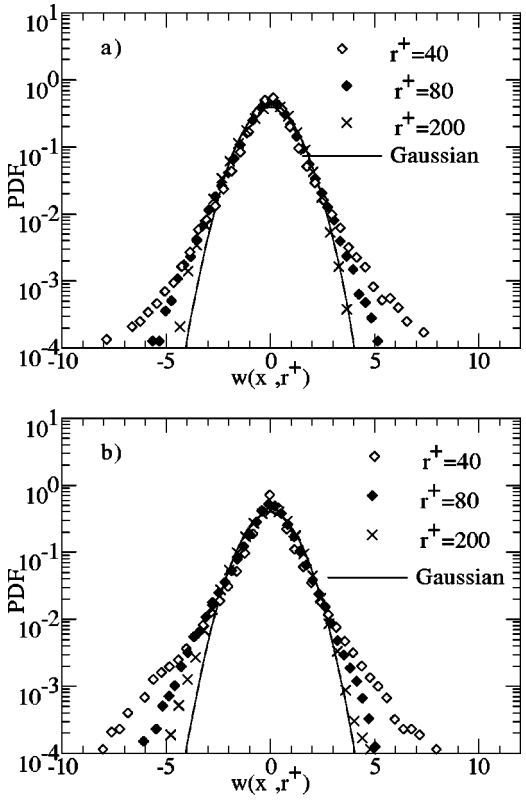

FIG. 7. Probability density function of the wavelet coefficients at $y^+=310$ (a), and $y^+=15$ (b), for scale $r^+=40$, $r^+=80$, and $r^+=20$, in semilogarithmic coordinate. The PDF are centered and normalized such that the area underneath each is unity.

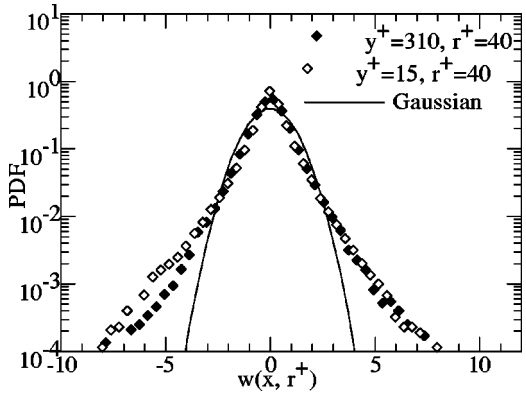

FIG. 8. Probability density function of the wavelet coefficients at $y^+=310$, and $y^+=15$, for scale $r^+=40$, in semilogarithmic coordinate. The PDF are centered and normalized such that the area underneath each is unity.

B. Conditional analysis and bursting effects

The eduction method developed and described in the Sec. I(C) has been used to analyze the velocity signals and to track events. The present approach, being based on wavelet decomposition, permits the effects of organized structures to be better evidenced even if the background turbulence energy level is much higher than the energy associated to the intermittent structures. Furthermore, with the present technique the contribution to intermittency for different scales may be analyzed due to the selectivity nature of the wavelet decomposition, and the ambiguity in the choice of the threshold for the events selection is avoided.

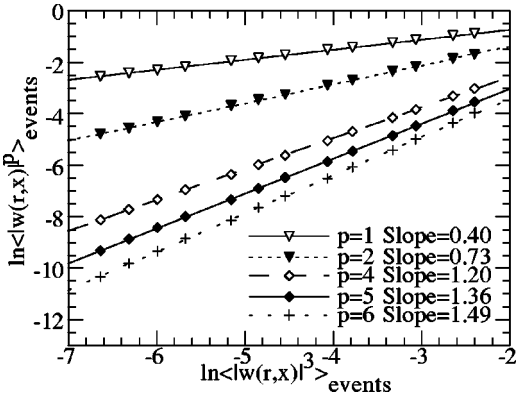

FIG. 9. Moments from 1 to 6 of the wavelet coefficients as a function the third order moment conditioned on the nonbursting part of the signal. The slope of the fits represented by lines are reported.

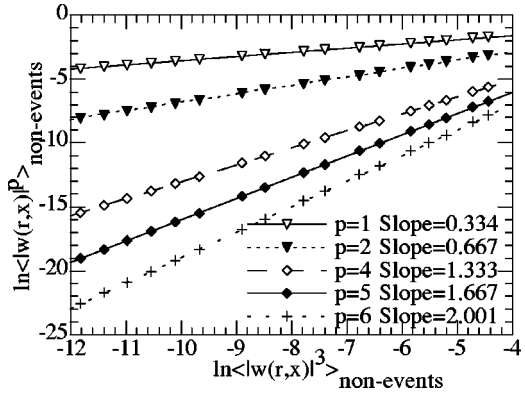

FIG. 10. Moments from 1 to 6 of the wavelet coefficients as a function the third order moment conditioned on the bursting part of the signal. The slope of the fits represented by lines are reported.

In order to test numerically the eduction method and to confirm that the events educed are really responsible for the anomalous scaling, we compute scaling exponents first considering only the events, Fig. 9, and then excluding the events, Fig. 10. The exponents are computed using the ESS for the wavelet transform, averaging only on the coefficients corresponding, respectively, to the events and to the nonevents. The scaling exponents are reported in Table III. A linear scaling is found for the nonevent region whereas an anomalous scaling, with exactly the same scaling exponents as those obtained by the complete signal is found for the events (see Table I).

The results of Table III therefore confirm that the structures associated with the detection method here developed are responsible for the observed anomalous scaling. Indeed, when such events are eliminated, intermittency anomalies are no longer observed and the Kolmogorov prediction is achieved. The procedure adopted for the threshold selection seems therefore to be capable of separating a strongly non-Gaussian contribution with anomalous scaling from the quasi-Gaussian background of the turbulent flow whose scaling exponents are a linear function of p.

According to the phenomenology described above, the number of events should be greater close to the wall because of the bursting activity. In Fig. 11 we show the number of detected events per unit length in wall unit, n^+, at $y^+=15$, 28.8, 103, and 310, as a function of the wavelet scale where the eduction scheme is applied. The number of events is about the same, almost zero, for scales greater than $r^+=200$. For smaller scales, the number of events starts growing quickly in the buffer layer ($y^+=15, 28.8$) while in the logarithmic region ($y^+=103$) and close to the center of the channel ($y^+=310$), the number of events is lower. These results are consistent with the ones obtained previously through the structure function analysis indicating the stronger intermittency of the buffer layer with respect to the other regions.

TABLE III. Scaling exponents at $y^+=15$ conditioned on the events and conditioned on the nonevents.

p	$\zeta_p y^+=15$ events	$\zeta_p y^+=15$ nonevents
1	0.40	0.334
2	0.73	0.667
3	1.00	1.000
4	1.20	1.333
5	1.36	1.667
6	1.49	2.001

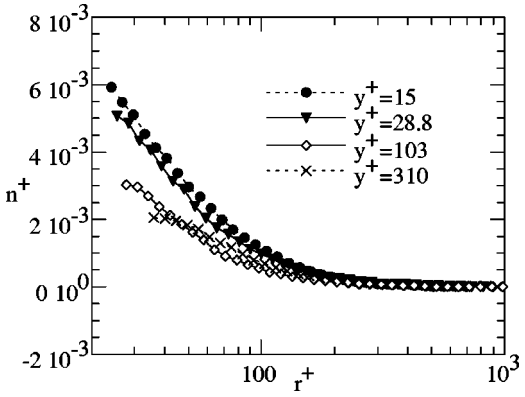

FIG. 11. Number of educed events per unit length in wall units as a function of wavelet scale r^+ for $y^+=15$, 28.8, 103, 310.

So far, we have shown that the number of events is greater in the buffer region but their mean shape has not yet been discussed. Indeed, according to previous analyses (e.g. Ref. [14]) the dynamics of the coherent structures should generate high velocity gradients. In Fig. 12 the averages of the streamwise velocity conditioned on the educed events are shown for $y^+=15$ in the case of accelerated event (we used the Taylor hypothesis, so accelerating events in time correspond to decelerating events in space). The two curves correspond to two different scales, $r^+=40,80$, used for the I computation and for the selection of the set of instants for the ensemble averaging. The figure confirms that events selected by the educing technique consist of strong velocity gradients which are found at all scales.

More detailed information on the shape and topology of the wall organized motion responsible for the mean time signatures observed in Fig. 12 cannot be achieved by present pointwise measurements. This aspect remains a task for future development.

IV. FINAL REMARKS AND CONCLUSIONS

In this paper, an experimental study of the intermittency effects on the statistics of the pointwise longitudinal velocity

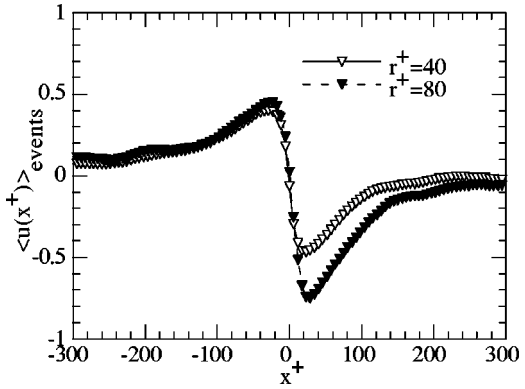

FIG. 12. Conditional average over the accelerated events of the streamwise velocity component at $y^+=15$ for $r^+=40$ and $r^+=80$.

signals acquired in a turbulent channel flow, has been presented.

The statistical analysis has been performed using different indicators, and the study has been conducted both on the velocity structure functions and on the wavelet coefficients obtained by the decomposition of the velocity time series. For a careful analysis of the turbulent flow considered, a unique technique for events eduction has been developed. The method substantially extends a previous identification scheme based on the wavelet decomposition of the velocity signals [22]. In the present approach the uncertainties related to the choice of the threshold level for events selection are eliminated: the threshold is selected as a separation level between quasi-Gaussian and non-Gaussian contribution to the velocity signal as a whole. The analysis has been applied to pointwise velocity signals acquired by a single hot wire probe at distances from the wall ranging from $y^+=7$ up to $y^+=310$.

The present results have shown that the region in which the small scale intermittency is stronger corresponds to the buffer layer. This result has been achieved by the analysis of the relative scaling exponents obtained by the ESS form of scaling and by the computation of the PDF of the wavelet coefficients. It has been found that for positions close to the channel centerline ($y^+=310$), scaling exponents are in substantial agreement with previous observations in homogeneous and isotropic turbulence, whereas for $10\leqslant y^+\leqslant 40$ corresponding to the buffer layer, they increase significantly and the PDF's tails enlarge. We have developed and applied on the streamwise velocity component an eduction technique based on the wavelet transform. It has been shown that the events selected by the present technique are responsible for the anomalous scaling observed on the velocity (or wavelet) structure functions. This point has been addressed by the analysis of the ESS computed from the signals conditioned on the selected events. Specifically, when the events are removed, nonintermittent scalings are observed. It has also been shown that the number of events increases moving towards the wall. From this analysis it appears that the bursting process, typical of a turbulent boundary layer, gives a strong contribution to the intermittency process. Moreover, even though from the present analysis detailed topological information is not available, the mean structures obtained by enseamble averages of the streamwise velocity conditioned on the educed events are associated to velocity gradients.

ACKNOWLEDGMENTS

The authors wish to acknowledge R. Verzicco for helpful comments. G.I. and R.C. were partially supported by MURST.

[1] U. Frisch, *Turbulence: The Legacy of A. N. Kolmogorov* (Cambridge University Press, Cambridge, UK, 1995).
[2] F. Anselmet, Y. Gagne, E.J. Hopfinger, and R.A. Antonia, J. Fluid Mech. **140**, 63 (1984).
[3] A. Arneodo, *et al.*, Europhys. Lett. **34**, 411 (1996).
[4] A. Vincent and M. Meneguzzi, J. Fluid Mech. **225**, 1 (1991).
[5] E.D. Siggia, J. Fluid Mech. **107**, 375 (1981).
[6] Z.S. She and E. Léveque, Phys. Rev. Lett. **72**, 336 (1994).
[7] A.K.M.F. Hussain, J. Fluid Mech. **173**, 303 (1986).
[8] R. Camussi, D. Barbagallo, G. Guj, and F. Stella, Phys. Fluids **8**, 1181 (1996).
[9] B. Protas, S. Goujon-Durand, and J.E. Wesfreid, Phys. Rev. E **55**, 4165 (1997).
[10] E. Gaudin, S. Goujon-Durand, J. Wojciechowski, and J.E. Wesfreid, Phys. Rev. E **57**, R9 (1997).
[11] F. Chillá and J.F. Pinton, in *Advances in Turbulence VII*, edited by U. Frisch (Kluwer, Dordrecht, 1998), pp. 211–214.
[12] G. Amati, F. Toschi, S. Succi, and R. Piva, *Advances in Turbulence VII* (Ref. [11]), pp. 159–162.
[13] R.A. Antonia, P. Orlandi, and G.P. Romano, Phys. Fluids **10**, 3239 (1998).
[14] J. Jeong, F. Hussain, W. Schoppa, and J. Kim, J. Fluid Mech. **332**, 185 (1997).
[15] J. Jimenez and A. Pinelli, J. Fluid Mech. **389**, 335 (1999).
[16] V.A. Sandborn, J. Fluid Mech. **6**, 221 (1959).
[17] D.A. Shah and R.A. Antonia, Phys. Fluids A **1**, 318 (1989).
[18] D. Britz, D.A. Shah, and R.A. Antonia, Phys. Fluids **31**, 1431 (1988).
[19] K.R. Sreenivasan, J. Fluid Mech. **151**, 81 (1985).
[20] R. Benzi, S. Ciliberto, R. Tripiccione, C. Baudet, F. Massaioli, and S. Succi, Phys. Rev. E **48**, 29 (1993).
[21] M. Farge, Y. Guezennac, C.M. Ho, and C. Meneveau, *Proceedings of the Summer Program 1990*, (CTR, Stanford, 1990).
[22] R. Camussi and G. Guj, J. Fluid Mech. **348**, 177 (1997).
[23] Z.S. She, E. Jackson, and S.A. Orszag, Nature (London) **344**, 226 (1990).
[24] R. Benzi, L. Biferale, S. Ciliberto, M.V. Struglia, and R. Tripiccione, Physica D **96**, 162 (1996).
[25] S. Grossmann, D. Lohse, and A. Reeh, Phys. Rev. E **56**, 5473 (1997).
[26] A. Kolmogorov, C. R. Acad. Sci. URSS **30**, 301 (1941).
[27] M. Farge, Annu. Rev. Fluid Mech. **24**, 395 (1992).
[28] G.G. Katul, M.B. Parlange, and C.R. Chu, Phys. Fluids **6**, 2480 (1994).
[29] G. Iuso, Aeronaut. J. **98**, 388 (1994).
[30] P.M. Ligrani and P. Bradshaw Exp. Fluids **98**, 407 (1987).
[31] M. Briscolini and P. Santangelo, J. Fluid Mech. **270**, 199 (1994).
[32] R. Camussi, C. Baudet, R. Benzi, and S. Ciliberto, Phys. Rev. E **54**, R3098 (1996).
[33] R.A. Antonia, M. Teitel, J. Kim, and L.W.B. Browne, J. Fluid Mech. **236**, 57 (1992).
[34] Data taken from CD ROM attached to Advisory Group for Aerospace Research & Development Advisory Report No. AGARD-AR-345 (NATO, April 1998).
[35] P.H. Alfredsson and A.V. Johansson, J. Fluid Mech. **9**, 325 (1984).
[36] R.A. Antonia, T. Zhou, and G.P. Romano, Phys. Fluids **9**, 3465 (1997).
[37] R. Benzi, G. Amati, C.M. Casciola, F. Toschi, and R. Piva, Phys. Fluids **11**, 1284 (1999).